Journal of Mathematical Chemistry 14 (1993) 153–174

The dsd model in heptacoordinate stereochemistry: a comparison with experiment

J. Brocas

Chimie Organique, Faculté des Sciences, Université Libre de Bruxelles, 50 avenue F.D. Roosevelt, B-1050 Bruxelles, Belgium

Received 27 March 1992

The diamond–square–diamond or dsd model provides a simple description for heptacoordinate interconversion. We compare it to NMR information. It appears that the model is almost always compatible with experimental facts, at least when the dsd processes do not lead to isomerization.

1. Introduction

It is generally admitted that heptacoordinate static stereochemistry may be discussed in terms of three geometrical structures: D_{5h} pentagonal bipyramid, C_{2v} 4-capped trigonal prism and C_{3v} capped octahedron [1]. The C_s tetragonal base-trigonal base or 4 : 3 geometry has also been proposed [1]. Deformations leading to interconversions between D_{5h}, C_{2v} and C_{3v} have been described and their relation to dynamic stereochemistry of heptacoordinate complexes has been assumed [2].

Since this pionneer work, important progress has been accomplished. In spite of this, heptacoordination remains poorly understood in its static and dynamic aspects, when compared to penta- or hexacoordination. There are two reasons to be invoked: first, there exists no regular polyhedron with seven vertices which could be used as a reference static structure and, second, there exist 34 polyhedra with seven vertices, compared to two with five vertices and seven with six vertices [3,4].

It seems therefore suitable to simplify the description of the heptacoordinate stereochemistry, even if discrepancies from any simple model are to be expected. The proposal of King [4,5] is based on a very elegant work of Lipscomb on boranes and carboranes [6]: among the n-vertex polyhedra representing a given ML_n complex, those having only triangular faces (deltahedra) are assumed to be energetically favoured. The so-called single dsd processes, since they involve removal and subsequent addition of one edge, are also favoured because only two triangular

faces are lost and replaced by only one quadrilateral face in the intermediate state. Degenerate dsd play a special role since the starting and final polyhedron are identical up to a permutation or a permutation–inversion of the vertices (vide infra). Single degenerate dsd are not always possible. Hence, double degenerate dsd (or even triple, ...) may be the simplest degenerate dsd's (two or three edges are then switched). Of course, the better stability of deltahedra is not an absolute rule, since calculations based on the minimization of the total repulsion of the ML bonds, lead to the conclusion that the C_{2v} 4-capped trigonal prism (a non-deltahedron) is of comparable stability as the C_{3v} capped octahedron and the pentagonal bipyramid (two deltahedra) [7]. Hence, the dsd description is not expected to be an absolute rule either, but rather a first approximation in terms of which possible exceptions have to be discussed.

The aim of this paper is to compare systematically experimental results, specifically NMR line shape analysis, to the prediction of the dsd model. Therefore, we use the permutational description of the dsd mechanisms, derived previously [8]. In this recent work, we have analyzed single and double degenerate dsd for the five heptacoordinate deltahedra in terms of the modes of rearrangements [9–11]. The results of this comparison for two of these deltahedra, namely the pentagonal bipyramid and capped octahedron, are given in sections 2 and 3 respectively. The 4 : 3 "piano stool" geometry is discussed in section 4, where dsd mechanisms for this geometry are described. In section 5, the experimental behaviour of complexes of 4-capped trigonal prismatic structure is compared to the dsd model for this polyhedron, which is detailed in the appendix.

2. The pentagonal bipyramid

We first recall the well-known dsd mechanism for the pentagonal bipyramid. It interconverts pentagonal bipyramids via 4-capped trigonal prismatic intermediates [2,4,6]. It has been shown that this is the only possible dsd process for pentagonal bipyramids [8]. This double degenerate dsd is represented in fig. 1. The crosses denote the switching edges. The symbol # refers to the polyhedra numbers used by

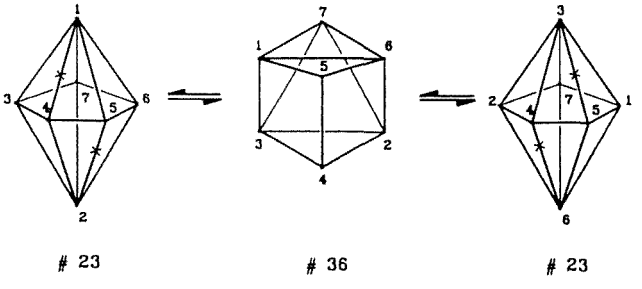

Fig. 1. Double degenerate dsd for the pentagonal bipyramid.

King [4]. The correspondence between these numbers and those of ref. [3] may be found in ref. [8].

Some previous experimental results show agreement with this mechanistic proposal; the dynamic behaviour of other systems is incompatible with this model.

2.1. TRISCHELATES

The structures of $Mo(NO)(S_2CNMe_2)_3$ [12], $Mo(N_2R)(S_2CNMe_2)_3$ (R = aryl), $TiCl(S_2CNMe_2)_3$ [13] are analogous: the monodentate ligand is in axial position, two chelates occupy equatorial positions and the third chelate is axial–equatorial. A similar structure holds for $TiCl(SOCNR_2)_3$ (R = Me, Et) [14] where the three chelate sulfur atoms are on the same triangular face of the trigonal bipyramid. The complexes with symmetrical chelates have four kinds of methyl groups at low temperature (ratio 2 : 2 : 1 : 1) and show a single methyl peak at high temperature. These results have been discussed in terms of various mechanisms including interconversion between pentagonal bipyramid and end capped trigonal prism [12,13]. The complexes with unsymmetrical chelates show two distinct processes:

(1) a low temperature process exchanging equatorial and axial–equatorial chelates possibly through a capped octahedral intermediate,

(2) a high temperature one involving rotation about the chelate C–N bonds [14].

For all these complexes, the only double degenerate dsd (fig. 1) leads to an isomer where the unidentate ligand is no longer in apical position. Since such an isomer has not been observed, this double dsd does not seem to arise in these systems.

Another trischelate, $TaX(\eta^4\text{-naphthalene})(dmpe)_2$ (dmpe = $Me_2PCH_2CH_2PMe_2$), will be discussed below since its dynamical behaviour is similar to that of some parent bischelates.

2.2. BISCHELATES

In the seven-coordinate complex $Ta(NMe_2)_2(O_2CNMe_2)_3$, one NMe_2 ligand and two bidentate O_2CNMe_2 chelates occupy the equatorial plane [15]. The other NMe_2 and the third O_2CNMe_2 – a monodentate ligand – are in axial positions. Detailed ^1H and ^{13}C NMR analyses show that, above 0°C, the O_2CNMe_2 ligands become equivalent and the NMe_2 signals also coalesce. This process involves not only the seven-coordinate TaN_2O_5 moiety but also one of the O atoms of the dangling ligand. Since this is an eight-site exchange process, we do not discuss it further.

In $TaH[P(C_6H_5)_2]_2(dmpe)_2$, the PPh_2 ligands are apical and the equatorial sites are occupied by the H and the two dmpe ligands [16], an approximate C_{2v} structure. The dmpe methyl groups are either adjacent or opposite to the hydride ligand, leading to the distinct ^1H resonances at room temperature. At 80°C, these resonances coalesce. The proposed mechanism involves interconversion between pentagonal bipyramid and a capped octahedron, with H as capping ligand and trans PPh_2

ligands [#1]. This can be viewed as a non-degenerate single dsd. Coalescence of the methyl signals is achieved via migration of H about the octahedral faces. Again, the mechanism of fig. 1 transforms the ground state structure with apical PPh_2 into an unobserved isomer with equatorial PPh_2. Hence, the dsd does not seem compatible with the observed behaviour of this complex.

Instead of the chelates occupying equatorial sites as in the previous example, they can also span two axial–equatorial sites. This is for instance the case with $ReH_3(L\text{–}L)_2$ (here L–L is dppe = $(C_6H_5)_2PCH_2CH_2P(C_6H_5)_2$ or dpae $(C_6H_5)_2AsCH_2CH_2As(C_6H_5)_2$), where two of the three hydrogens occupy adjacent equatorial positions, the third one being adjacent to the two equatorial phosphorus or arsenic atoms [18]. This is a C_2 static structure (see fig. 2).

At room temperature, the ^1H spectrum in the hydride region of these compounds indicates that the three hydrides are equivalent. At −50°C, only two of the hydride ligands show equivalence, in agreement with the proposed structure. However, for the $ReH_3(dppe)_2$ complex, at this temperature, the four P atoms appear to be equivalent. This could be realized by a double degenerate dsd (or pairwise exchange) where the suppressed edges are either 16 and 47 or 17 and 46 (see fig. 2). The permutation–inversion representing these events are $x = (12)(34)(67)J$ or $y = (13)(24)(67)J$ respectively. Note that x and y contain the inversion about the center of mass, J. Indeed, in fig. 2 the chirality of the non-centrosymmetric skeleton is inversed.

The analysis of the hydride coalescence could be performed in terms of the group

$$H \equiv C_2 = [I, (14)(23)(67)],$$

which is the group leaving the effective spin Hamiltonian of the static structure invariant (ref. [11]) and references cited therein) and taking into account the genera-

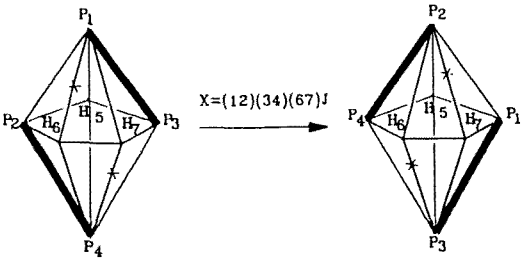

Fig. 2. $ReH_3(dppe)_2$, the double degenerate dsd. The heavy lines represent chelate bridges.

[#1] This mechanism is the same as the $D_{5h} \rightarrow C_{3v} \rightarrow C_{2v}$ path with retention of a mirror plane [17]. It has a common feature with the dsd process of fig. 1: both lead from D_{5h} to C_{2v}, the transition state of the dsd. However, in the $D_{5h} \rightarrow C_{3v} \rightarrow C_{2v}$ path one of the axial ligands in D_{5h} becomes the capping ligand in C_{2v}. This is not the case in the dsd process.

tors x or y of the assumed dsd low temperature mechanism. The resulting non-rigid group is (when x is used)

$$H_{NR} = [I, (14)(23)(67), (12)(34)(67)J, (13)(24)J]$$

instead of the C_{2v} group used previously [18],

$$C_{2v} = [I, (14)(23)(67), (14), (23)(67)] .$$

Capped octahedra have been invoked as intermediates on the pathway leading to hydride coalescence [18].

A more detailed mechanistic investigation has been performed for $TaX(\eta^4$-naphthalene)$(dmpe)_2$ (dmpe = $Me_2PCH_2CH_2PMe_2$) [19]. This trischelate is rather similar to the $ReH_3(dppe)_2$ bischelate: the naphthalene chelating unit is ligated in such a way that its complexed 1,3-diene moiety plays the role of the two neighbouring hydrides in fig. 2. The remaining uncomplexed benzene ring (symbolized by a half circle in fig. 3) lies above or below the equatorial plane.

The experimental results, i.e. ^{31}P NMR line shape analysis, are best explained by the double degenerate dsd of the pentagonal bipyramid (see fig. 1). Its application to the present case is shown in fig. 3. In this figure, the transformations denoted by k_1 and k_2 invert the chirality of the complex; the crosses and circles denote the edges which are switched in the k_1 and k_2 transformations, respectively. The transition states of these transformations are both 4-capped trigonal prisms, with X as the capping ligand and the naphthalene on the edge shared by the two

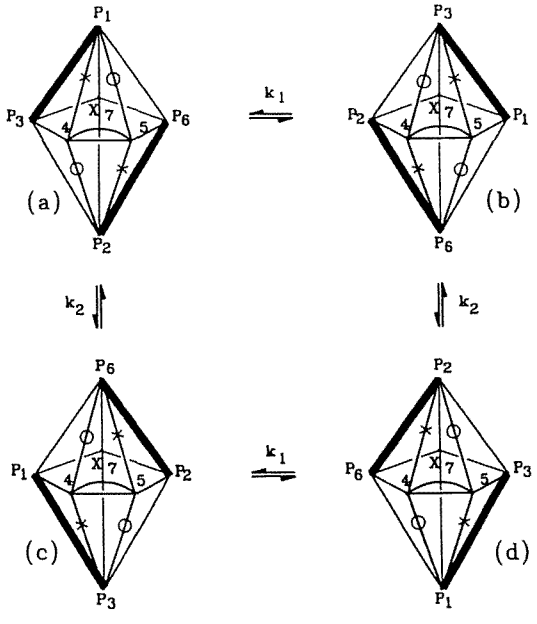

Fig. 3. Degenerate double dsd for $TaX(\eta^4$-naphthalene)$(dmpe)_2$.

quadrilateral faces. The dmpe chelates are on opposite edges of the capped face. The symmetry plane of these C_s transition states is perpendicular to the dmpe edges in the case of the k_1 transformation, but parallel to these edges for the k_2 transformation.

2.3. MONOCHELATES

Instead of the double degenerate dsd or pairwise exchange displayed by the above two complexes, let us now discuss an example of non-pairwise exchange. The complex $HMo[P(OCH_3)_3]_4[O_2CCF_3]$ [20] is an approximate pentagonal bipyramid. Two phosphite ligands are axial and the two other are separated by the hydride ligand in the equatorial plane. The trifluoroacetate chelate is also equatorial. The solid-state geometry is distorted towards a capped octahedron since the hydride ligand is displaced from the equatorial plane. The solution structure observed by ^1H NMR at $-100°C$ is consistent with an averaged C_{2v} geometry due to rapid tunnelling of the hydride ligand through the equatorial plane. Distinction between the axial and equatorial phosphorus vanishes above $-20°C$. This coalescence could be due to the pairwise exchange or double dsd discussed previously. But lineshape analysis shows that the experimental coalescence pattern is compatible with non-pairwise exchange and not with pairwise or degenerate double dsd exchange.

2.4. MONODENTATE LIGANDS

The $CrH_2[P(OCH_3)_3]_5$ complex [21,22] is a pentagonal bipyramid where the hydride ligands are in equatorial position. On the basis of H–H coupling constant, the proximal structure [21] (with the two hydrides in neighbouring positions) has been ruled out [22] and distal structure is assumed (see fig. 4).

The permutational analysis of the ^{31}P and ^1H NMR coalescence pattern has been performed [22]. We give here an equivalent presentation, based on NMR-modes and modes of rearrangements [9–11]. The group permuting the five P atoms and the two H ligands, i.e. $S = S_5(12345) \times S_2(67)$ may be decomposed into NMR-modes:

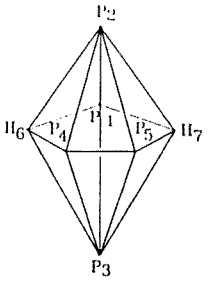

Fig. 4. Labelling of $CrH_2[P(OCH_3)_3]_5$.

$$M_{\mathrm{NMR}}(x_i) = Hx_iH\,.$$

Here

$$H = [I, (23)(45)(67), (23)(45)(67)]\,.$$

Using standard group theoretical methods (see ref. [11]) for details), it is easy to show that there exist 19 such NMR-modes. When an NMR-mode is not self-inverse [23,24] it has to be replaced by an extended NMR-mode [11],

$$M^{\mathrm{ext}}_{\mathrm{NMR}}(x_i) = (Hx_iH) \cup (Hx_i^{-1}H)\,,$$

where $\cup$ means "union". In the present case, thirteen NMR-modes are self-inverse and the remaining six consist of three pairs of mutually inverse NMR-modes. Hence there are sixteen NMR-modes or extended NMR-modes, in one to one correspondence with the sixteen basic permutational sets (BPS) discussed in ref. [22] for the analysis of the phosphorus–proton spin system. Only two BPS are compatible with the experimental coalescence patterns. They correspond to the NMR-modes $M_{\mathrm{NMR}}(x_9)$ and $M_{\mathrm{NMR}}(x_{10})$ listed in table 1 (see ref. [22]).

The notion of mode of rearrangement is relevant for the mechanistic discussion. Such a mode is the set of permutations describing pathways which must occur with the same probability and/or lead to the same configuration starting from a given one [9–11]. It is defined as follows:

$$M(y_i) = (Ay_iA) \cup (A\sigma y_i\sigma^{-1}A)\,.$$

Here the group of proper operations is

$$A = [I, (23)(45)(67)]\,,$$

whereas σ is any improper operation, e.g. $\sigma = (23)$. In the present case, the two relevant NMR-modes consist each of two modes of rearrangements. In table 1, the vertical line separates different modes of rearrangements of a given NMR-mode, while the symbols A, B, C, D are those of Van-Catledge, Ittel and Jesson [22]. These authors have used a quasi-least-motion method to generate reaction pathways for

Table 1
NMR-modes for $CrH_2[P(OCH_3)_3]_5$.

i	A	B	C	D
9	(13)(25)(67)	(13542)	(13)(254)	(1352)(67)
	(13)(24)(67)	(13452)	(13)(245)	(1342)(67)
	(12)(35)(67)	(12453)	(12)(345)	(1253)(67)
	(12)(34)(67)	(12543)	(12)(354)	(1243)(67)
10	(13)(25)	(13542)(67)	(13)(254)(67)	(1352)
	(13)(24)	(13452)(67)	(13)(245)(67)	(1342)
	(12)(35)	(12453)(67)	(12)(345)(67)	(1253)
	(12)(34)	(12543)(67)	(12)(354)(67)	(1243)

the eight possibilities (9A, 9B, 9C, 9D, 10A, 10B, 10C, 10D) of table 1. They find that only four of them (9AB, 9CD, 10AB, 10CD) are distinct, i.e. each mode of rearrangement generates a pathway in this method.

This result is easy to understand by using the PSD/TS method [24–27]. Indeed, assuming that the transition state (TS) is a simple saddle point directly linked to reactants and products by paths of steepest descent (PSD) [26] it is easy to construct $\tilde{A}$ and $\tilde{R}$ (the group of proper symmetry operations and the point group of the PSD) as well as A_T and R_T (the same groups for the TS) [27]. In this PSD-TS method, these four groups are characteristic of the mode of rearrangement:

(a) all the permutations of such a mode leading to the same configuration [11] generate the same set $\{\tilde{A}, \tilde{R}, A_T, R_T\}$,

(b) the groups $\{\tilde{A}, \tilde{R}, A_T, R_T\}$ obtained from different configurations of the same mode of rearrangement have different permutational expressions but identical geometrical meaning. This is why, in the present case, only four TS geometrical structures are found, assuming that PSD/TS methods leads to quasi-least-motion structures.

The results are given in table 2 for the four rearrangement modes compatible with the NMR results.

As it is seen from this table, the TS of 9AB and 10AB are both of C_2 symmetry. However, for 10AB, the two hydride ligands and P_4 are on the C_2-axis, a rather unrealistic geometry. This corresponds to the finding that the hydrides became nearly coincident in the quasi-least-motion approach [22]. Similarly, table 2 shows that the TS of 9CD and 10CD are of C_s symmetry, since the presence of J corresponds to an improper operation [27,28]. Geometries compatible with these TS are shown in fig. 5. They are in agreement with those proposed by Van-Catledge, Ittel and Jesson [22]. The symmetry of these TS is lower than the symmetry (C_{2v}) of the corresponding graphs, due to the presence of the hydride ligands. As a consequence, edges may be added to these polyhedra without lowering the TS symmetry. For instance an edge 13 (or 67) may be added to the TS of 9AB; the edges 27 and 23 (or 56 and 15) to the TS of 9CD; the edges 26 and 56 (or 34 and 14) to the TS of 10CD. This last TS is in fact the 4-capped trigonal prism of the degenerate double dsd of the pentagonal bipyramid, one of the mechanisms compatible with the NMR results of $CrH_2[P(OCH_3)_3]_5$.

Table 2
PSD and TS groups

Mode	$\tilde{A}$	$\tilde{R}$	A_T	R_T
9AB	I	I	I, (13)(25)(67)	I, (13)(25)(67)
9CD	I	I	I	I, (13)(25)(67)J
10AB	I	I	I, (13)(25)	I, (13)(25)
10CD	I	I	I	I, (13)(25)J

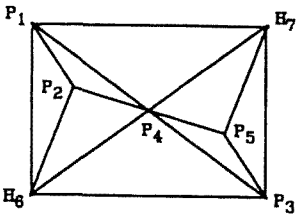

9AB

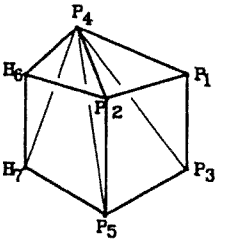

9CD

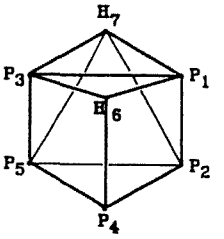

10CD

Fig. 5. Geometries compatible with the TS.

3. The capped octahedron

There are four double degenerate dsds for this geometry [8]. They are presented in fig. 6. In fig. 6(A) the well-known capped octahedron–4-capped trigonal prism transformation is shown [2,6].

In figs. 7 and 8 we represent various substitution patterns of the capped octahedron for which NMR information is available.

The structures shown in fig. 7 have been studied by ^{1}H and ^{13}C NMR [29]. The view is along the C_3 axis of the framework. The central metal is W in (A) and Mo in (B), (C), (D), (E), the heavy As–As lines stand for the cis-$(CH_3)_2AsC(CF_3) = C(CF_3)As(CH_3)_2$ bidentate chelate and P represents the phosphorus atom of $P(OCH_3)_3$ or $P(OCH_3)_2(C_6H_5)$ in (B) of $P(OC_2H_5)_3$ in (C) and $P(CH_3)_2(C_6H_5)$ in (D) and (E). Note that (D) and (E) represent possible configurations of the same complex, both consistent with room temperature NMR data. The observed non-rigidity of these structures has been discussed and migration of the capping CO over the faces of the octahedron has been assumed.

In fig. 8, we represent $TaH(CO)_2[(CH_3)_2PCH_2CH_2P(CH_3)_2]_2$ (A) and $MoH(CO)_2(P\text{–}P^*)_2^+$ (B), where the heavy line P–P* is $R_2PCH_2CH_2ER'_2$ (R = R′ = Me, E = P or R = R′ = Ph, E = P or R = Me, R′ = Et, E = P or R = Me, R′ = Ph, E = P or R = R′ = Me, E = As or R = R′ = Ph, E = As or R = Ph, R′ = Me, E = As). The Ta complex [30] and the Mo complexes [31] have been studied by ^{1}H and ^{31}P NMR. The Ta complex has coalescence patterns in reasonable agreement

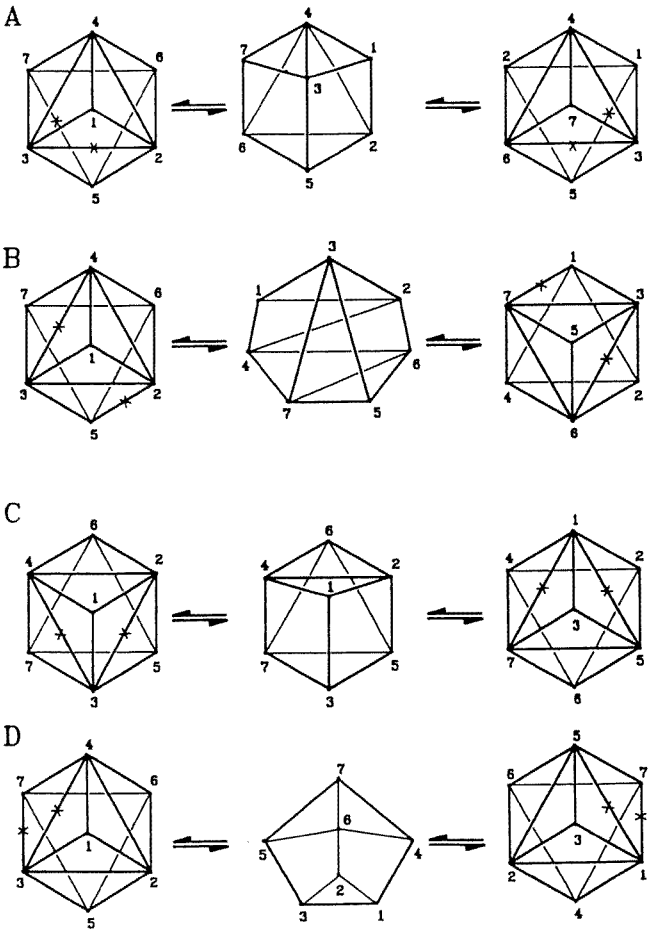

Fig. 6. Double degenerate dsd for the capped octahedron.

with those simulated for non-pairwise exchange of the chelate bridges, i.e. (12) or (34) (see fig. 8) describe this process. For Mo complexes, different behaviours are observed. For symmetric phosphines the spectra are compatible with pairwise exchange (i.e. (12)(34)) when R = R′ = Ph. Such an exchange may be realized via H migration from one octahedral face to another, on one side of the P4 plane, involving an undetected intermediate where the capped face has a chelate edge and a transition state of idealized pentagonal bipyramidal geometry. However, when R = R′ = Me a mixture of pairwise and non-pairwise exchange seems responsible for the observed spectral features. Migration of H between faces above and below the P4 plane has also been detected for the R = R′ = Ph symmetric phosphine. For various unsymmetric complexes, interconversion between cis and trans isomers has also been observed [#2].

[#2] In ref. [16], p. 4119, the complexes $MoH(CO)_2(P\text{–}P^*)_2$ are discussed in terms of D_{5h} instead of C_{3v} structure.

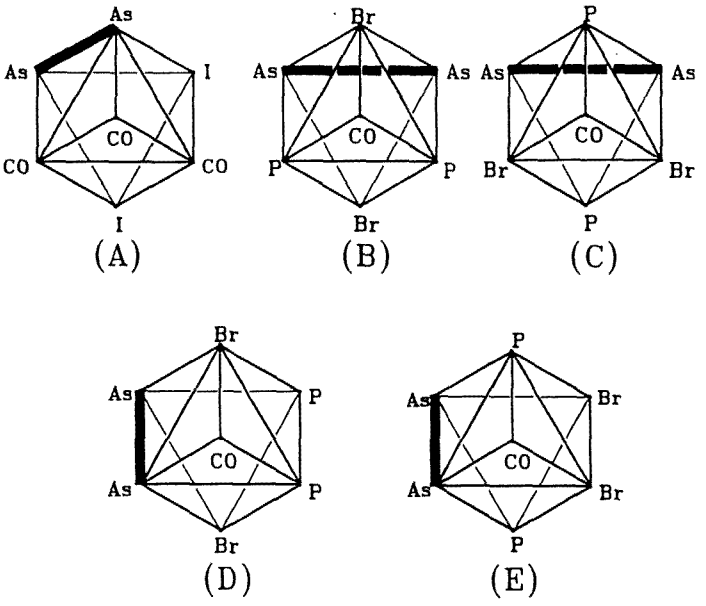

Fig. 7. Monochelate capped octahedra.

We now address the following question: are the dsd mechanisms of fig. 6 possible alternatives to the pairwise and non-pairwise exchanges? To answer this question, we first notice that the dsd mechanisms displace the capping ligand either to a site of the capped face (see fig. 6(C), (D)) or to a site of the opposite face (see fig. 6(A), (B)). As a consequence, when the capping group is the only one of this chemical species (i.e. CO in fig. 7(B), (C), (D), (E) and H in fig. 8(A), (B)), any of these dsd leads to an isomer distinct from the starting one. Since such isomerizations have not been detected, the dsd mechanisms are excluded for these complexes. The only complex for which a more detailed argument is necessary is shown in fig. 7(A). No isomerization has been detected for this molecule. Hence, dsd mechanisms where at least one of the COs is displaced to the opposite face (see fig. 6(A), (B), (C)) are incompatible with this observation. The only remaining

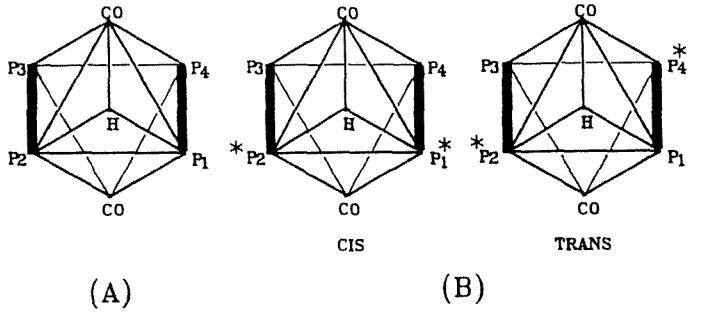

Fig. 8. Bischelate capped octahedra.

Fig. 9. A dsd for a monochelate capped octahedron.

dsd is that of fig. 6(D). It is represented by the permutation (14653): its effect on the tricarbonyl complex of fig. 7(A) is shown in fig. 9, where it is seen that it also produces an unobserved isomerization. Hence no dsd is compatible with the experimental results about capped octahedral complexes [#3].

4. The 4 : 3 piano-stool geometry

The 4 : 3 piano-stool geometry has been discussed by various authors (see for instance refs. [1,7,32–34]). It is characterized by the following features:

(i) the polyhedron has only one tetragonal face,

(ii) this tetragonal base is parallel to one of the triangular faces (the trigonal base) [33,34].

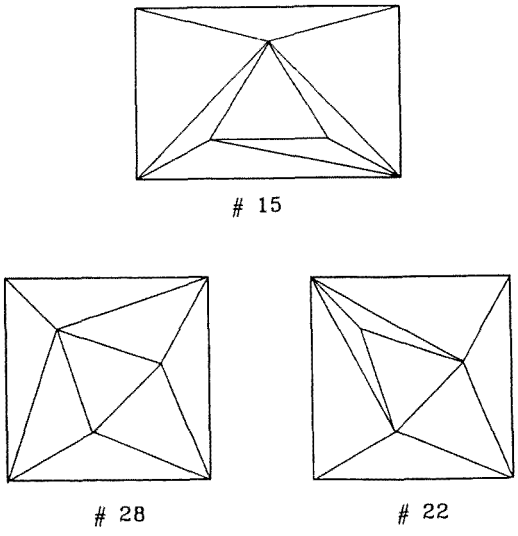

Fig. 10. Possible 4 : 3 polyhedra.

[#3] Similar arguments may be used to show that the dsd mechanisms lead to unobserved isomerization of $ReH_3[(C_6H_5)_2PCH_2CH_2O(C_6H_5)_2](PPh_3)_2$, a capped O_h molecule [18].

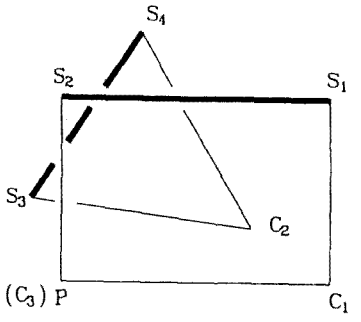

Fig. 11. A 4 : 3 structure.

These requirements do not specify unequivocally the polyhedron. Indeed, as shown previously [3] among the 34 polyhedra having seven vertices, eight have only one tetragonal face and three of them have a triangular face which does not touch the tetragonal one. These three polyhedra are shown in fig. 10, where the triangular base is under the tetragonal one. The graph symmetry of #15 is C_1 whereas #22 and #28 are C_s. It should be noted that a C_s symmetry where a trigonal base edge is parallel to a tetragonal base edge implies the existence of a second tetragonal face. Such a structure has been considered previously [1] but will not be discussed here since experimental data indicate that the complexes that we discuss below have only one tetragonal face [33,34].

The structure and dynamic properties of $W(CO)_3(S_2CNR_2)_2$ and $W(CO)_2L(S_2CNR_2)_2$ (R = Me, Et; L = PPh_3, PEt_3, $P(OEt)_3$) have been studied extensively [33,34]. The structure of the dicarbonyl derivative is shown in fig. 11. In the tricarbonyl complex, the phosphorus atom shown in fig. 11 has to be replaced by a third carbon monoxide carbon atom. In this figure, it is seen that the S atoms of the two N,N-dialkyldithiocarbamate chelates span one edge of the trigonal base and one of the tetragonal base. They are shown by heavy lines. However, in this figure, seven edges connecting the two bases are still missing. The edges PS_4, S_2C_2 and S_1S_3 are excluded since they lead to non-convex polyhedra. It is easy to show that there are four possibilities, shown in fig. 12, where the open circles and black dots refer to vertices of degree 3 and 5 respectively. The other vertices are of degree 4. It is seen that among the three polyhedra of fig. 10, only #22 and #28 are compatible with the experimental structure of fig. 11. The drawings denoted #28 (a), (b), (c) correspond to identical polyhedra but to different isomers, since the atoms S, P, C are disposed differently.

We first discuss the dicarbonyl derivative. The informations from NMR line shape analysis [34], show that at low temperature (−110°C), the two carbonyl carbons (C_1 and C_2) have different magnetic environments. The same is true for the central carbons of the dithiocarbamate chelates. The structures shown in fig. 12 are compatible with these experimental observations. At higher temperatures, a fluxional process equilibrates the central carbons of the chelates as well as the carbonyl

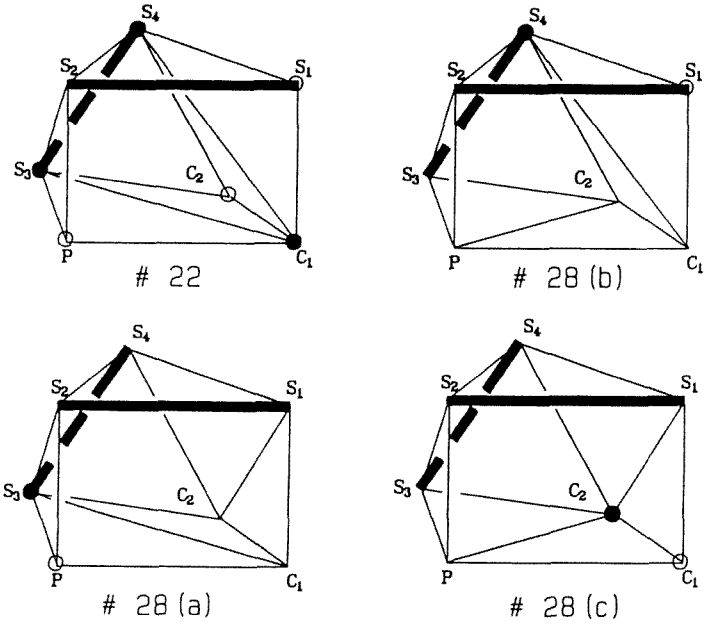

Fig. 12. Bischelate 4 : 3 polyhedra.

carbons. A mechanism has been proposed (scheme II, ref. [34]) to explain this NMR coalescence: the phosphine ligand is assumed to jump from the upper face SSC triangle to the lower face one (see fig. 11). However, in scheme II of ref. [34], some polyhedral edges have not been drawn. Since we are presently concerned with the possibility of describing this mechanism in terms of dsd processes, we have to examine the above jump for each of the structures shown in fig. 12, where all the edges are represented. For the structures #28(b) and (c), the above jump may be realized by suppressing the edge S_3C_2 and adding an edge S_2C_1. For #28(b), this gives rise to a structure where the degree of C_1 and C_2 are 3 and 5 respectively, instead of 4 for both C_1 and C_2 in the initial structure. Such an interconversion between different isomers is not observed experimentally. Hence, other edges have to be modified, in such a way that the initial and final structures are identical, up to a permutation, or a permutation inversion of atoms of the same species. This is shown in fig. 13.

In this figure, the crosses denote the edges which do not belong to the starting and the final structure. It is seen that in #28(b) and #28(c), two edge switchings occur on the diamond faces $S_1S_2S_3S_4$ and $S_1C_1C_2S_4$, a double dsd mechanism. The suppression of the edge S_3C_2 on the diamond face $PS_3S_4C_2$ and the addition of the edge S_2C_1 on the square face $PS_2S_1C_1$ is not – strictly speaking – a dsd process, since the initial and final diamond faces and the intermediate square faces do not involve the same vertices. We call it a dss'd' process (see appendix).

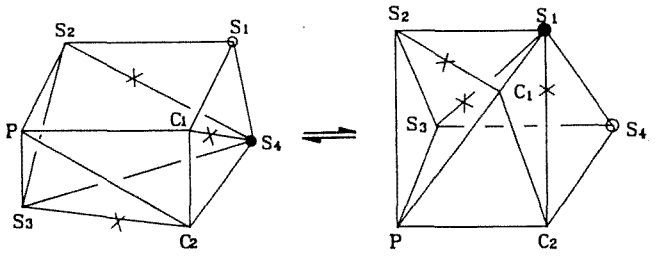

28 (b)

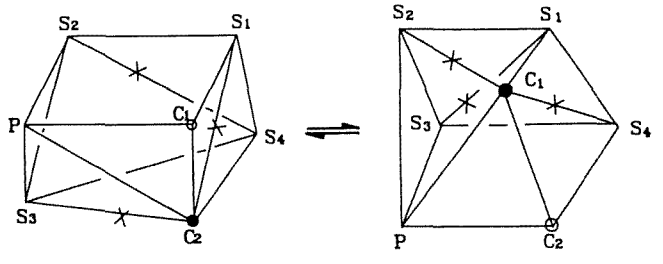

28 (c)

Fig. 13. Interconversion of 4 : 3 polyhedra.

So far, we only considered #28(b) and #28(c) in fig. 12. We now turn our attention to #22 and #28(a), two structures where the "jumping" phosphine ligand P is a vertex of degree 3. For this reason, the jump is only describable by suppressing and adding at least five edges. Since, such a process does not look very attractive, it will not be considered further.

We now discuss the tricarbonyl complex. At low temperature, the three carbonyl carbons are in different magnetic environments and the dithiocarbamate carbons are in two different environments [33]. In the intermediate temperature range, two carbonyl carbons (i.e. C_1 and C_3, see fig. 11) equilibrate. At higher tempera-

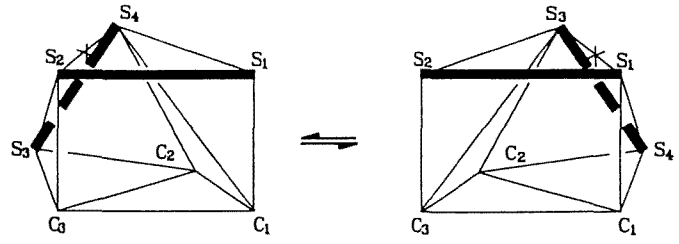

Fig. 14. Twisting motion on a 4 : 3 polyhedron.

ture, the three carbonyl carbons and the two chelate central carbons show each a single resonance.

The equilibration of the carbonyls C_1 and C_3 could be accounted for by a twisting of the trigonal base relative to the tetragonal base, as shown in scheme I of ref. [33]. In order to analyse such a motion in terms of eventual dsd mechanisms, we again use the structures of fig. 12 but this time the P atom has to be replaced by a third carbonyl denoted C_3 (see fig. 11). In fig. 14, the above twisting is performed on the tricarbonyl derivative of structure #28(b). It is seen that this motion induces a minimal modification of the edges of this 4 : 3 geometry. As shown by the crosses denoting the edges which are not common to the starting and final configurations, this motion is in fact a simple degenerate dsd. A similar discussion for tricarbonyl structures of type #22, #28(a) and #28(c) leads to more involved edge modifications and will not be considered further.

We now turn our attention to the high temperature equilibration of the tricarbonyl compound. The effective symmetry resulting from the intermediate range equilibration is that of the transition state of the twisting motion shown in fig. 14, i.e. a 4-capped trigonal prism, with C_2 as capping ligand (see fig. 15, left) [35]. The high temperature equilibration has been assumed to occur via a $2\pi/6$ rotation of the three carbonyl carbons (see scheme II of ref. [33]). The edge rearrangement corresponding to this process is shown in fig. 15. It is easy to realize that this process is in fact the dsd/dss'd' process shown in fig. 18.

5. The 4-capped trigonal prism

The possibility of fluxional behaviour of this polyhedron via dsd or analogous processes is discussed in the appendix. The results obtained there are now compared to those of NMR spectroscopy.

The compounds $[(t\text{-}C_4H_9NC)_7Mo]^{2+}$ and $[(t\text{-}C_4H_9NC)_6MoX]^{+}$ (X = Br, I) have 4-capped trigonal prism geometry with the halogen X in the capping site [7,35,36]. The $[Mo(CNR)_7]^{2+}$ shows only one ^{13}C resonance down to $-135°C$ [37], instead of the three signals expected for the static structure. This experimental

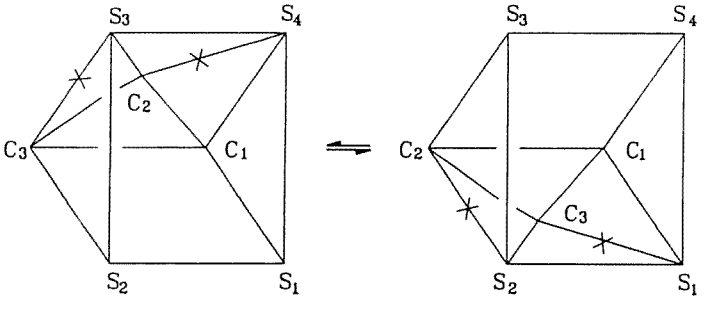

Fig. 15. Edge rearrangement in the TS of fig. 14.

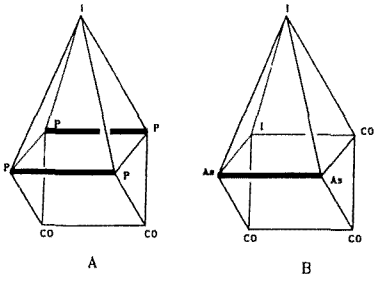

Fig. 16. Bischelate (A) and monochelate (B) of 4-capped trigonal prismatic structure.

fact is compatible with any of the modes of rearrangements [9–11] associated to the processes described in figs. 17–20. It is of course also compatible with other modes of rearrangements (see below) but allows no discrimination between these two possibilities.

The static structure of $[M(CO)_2(dmpe)_2I]^+$ (dmpe: 1,2-bis(dimethylphosphino) ethane, M = Mo, W) is shown in fig. 16(A), where the heavy lines represent the dmpe chelates [38]. At low temperatures, four of the eight methyl groups of the chelates are close to the capping I atom, while the four other are close to the CC edge, leading to distinct ^1H NMR signals. At room temperature, the eight methyl groups are equivalent. A similar behaviour has been observed for the chelate methylene groups. The assumed mechanism [38], a rapid migration of the I atom over all five faces of the P4C2 trigonal prism, implies the existence of three isomers (i) one with I capping the P4 face (ii) one with I capping a P2C2 face (iii) one with I capping a P2C face, while only one isomer (i) is observed. A remaining possibility is that (ii) and (iii) are high energy intermediates.

An alternative to this I migration has been proposed [39] in a study of cis–trans interconversion in $MX(CO)_2(L–L')_2$ (M = Mo, Ta; X = Cl, I; L–L': unsymmetric, bidentate phosphine). The labelled ends L and L' of the chelates span the capped face as in fig. 16(A) and interconversion between their cis and trans arrangements

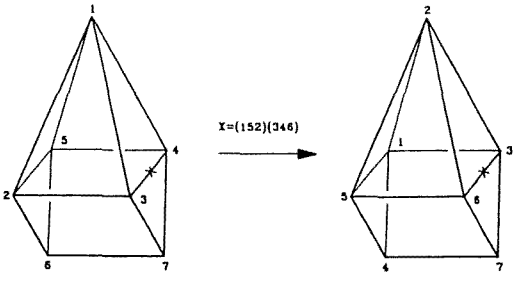

Fig. 17. A single degenerate dss'd' process.

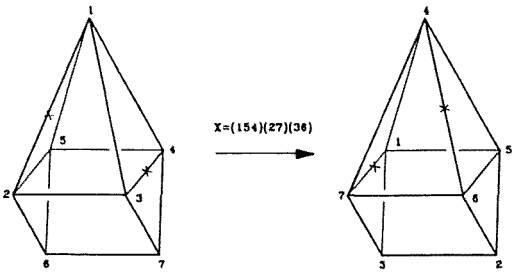

Fig. 18. A degenerate dsd/dss'd' process.

has been observed via ^{31}P and ^{1}H NMR. The detailed mechanism is a two-step process involving passage through a pentagonal pyramid, but the global effect is a twist of one of the chelates L–L'.

The role of dsd mechanisms in this cis $\rightleftharpoons$ trans transformation may be discussed either concerning the pentagonal pyramidal intermediate, or concerning the 4-capped trigonal prism. The former attitude has been developed in the original paper (see also section 2). The latter one rests on the possibilities of dsd for the 4-capped trigonal prism. It is seen in figs. 17–20 that any of these dsd's, when applied to the structure of fig. 16A, leads to an isomer where the halogen atom does no longer occupy the capping site. Since such isomers are not observed experimentally, we conclude that the dsd mecanisms of the 4-capped trigonal prism do not provide a good model for the fluxional behaviour of this systems.

A similar complex, $MoI_2(CO)_3[o\text{-}(As(CH_3)(C_6H_5))_2C_6H_4]$ is shown in fig. 16(B) [40]. Looking at figs. 17–20, we notice that the only dsd maintaining the position of the arsine bridging chelate is shown in fig. 20. However, this process sends the capping iodine towards one of the vertices of the edge which is parallel to the capped face, giving rise to an unobserved isomerisation. Hence the dsd processes of the 4-capped trigonal prism are not compatible with the behaviour of this derivative.

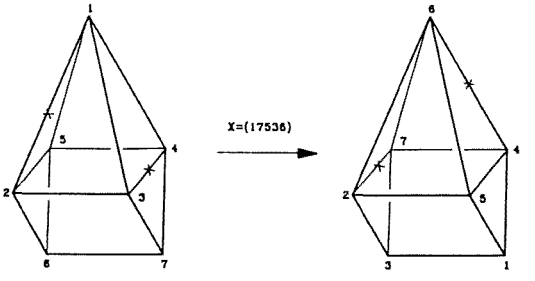

Fig. 19. A degenerate dss'd'/dss'd' process.

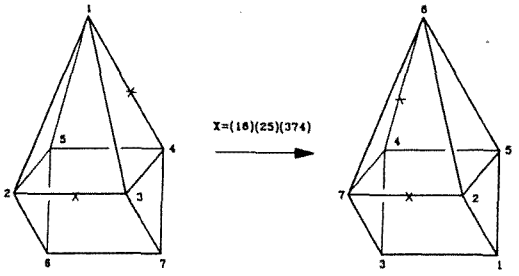

Fig. 20. A degenerate dss'd' 5-pyramidal process.

6. Conclusions

The conclusions about *capped octahedra* and *4-capped trigonal* prisms are quite clear: for these geometries the substitution patterns are such that the possible dsd pathways, when operative, should lead to unobserved isomerisations. The only exception is $[Mo(CNR)_7]^{2+}$, a 4-capped trigonal prism with seven identical monodentate ligands, but, unfortunately NMR information for this complex is compatible with any complete scrambling of the vertices. Hence, dsd pathways are excluded for these geometries, apart from $[Mo(CNR)_7]^{2+}$ [37]. The reason for this exclusion could come from the fact that the pathways themselves are unrealistic even for complexes with seven identical and monodentate ligands or from the fact that for the present particular substitution patterns the pathways generate unrealistic isomers, i.e. isomers distinct from the starting ones and for which electronic or steric requirements are not fulfilled [41].

It should, however, be noted that the dsd/dss'd' process shown in fig. 18 is compatible with the high temperature rearrangement of $W(CO)_3(S_2CNR_2)_2$, a 4 : 3 structure, via a 4-capped trigonal prism transition state of this complex (see fig. 15).

The situation is more complicated for *pentagonal bipyramids*, in spite of the fact that the only dsd process is the well-known D_{5h}–C_{2v}–D_{5h} traverse. For the trischelates $Mo(NO)(S_2CNMe_2)_3$, $Mo(N_2R)(S_2CNMe_2)_3$, $TiCl(SOCNMe_2)_3$, $TiCl(SOCNR_2)_3$, if the dsd process were to happen, it would transfer the monodentate ligand from an axial to an equatorial position, an unobserved and perhaps unfavourable isomerisation. Hence dsd is excluded for these complexes. It is also excluded for a similar reason in $TaH[P(C_6H_5)_2]_2(dmpe)_2$, a bischelate where the PPh_2 ligands are apical. However, the bischelates $ReH_3(dppe)_2$, $ReH_3(dpae)_2$ and the trischelate $TaX(\eta^4\text{-naphthalene})(dmpe)_2$ show a different behaviour: the three H ligands on the one hand and the X ligand and the (η^4-naphthalene) chelate on the other hand occupy non adjacent equatorial positions, whereas the remaining chelates are axial–equatorial. These three complexes have RMN coalescence patterns which are dsd compatible. For the monochelate, $HMo[P(CH_3)_3]_4[O_2CCF_3]$, the RMN coalescence pattern favours non-pairwise exchange and excludes double

degenerate dsd exchange, in spite of the fact that the last process can occur without leading to isomerization.

The 4 : 3 *geometry* shows also examples of dsd compatible pathways. A combination of a double degenerate dsd and a dss'd' process is equivalent to the jump of the L phosphine ligand in $W(CO)_2L(S_2CNR_2)_2$ (see fig. 13). The twisting motion of the tetragonal base via the trigonal base in $W(CO)_3(S_2CNR_2)_2$ is in fact a single degenerate dsd.

Finally, the general impression may be summarized as follows: the degenerate dsd have been defined for unsubstituted ML_7 complexes. The systems discussed above bear unequivalent and/or chelating ligands. In general this gives rise to only one stable observable isomer. This isomer may either be unvariant for the degenerate dsd's at hand or not.

If it is not invariant for the degenerate dsd, it will be transformed into another isomer by these processes. Since this isomer is unobserved, it is less stable and therefore the degenerate dsd is not feasible (except perhaps by multisteps via high energy intermediates). This does not mean that the pathway is itself unrealistic, but that the resulting isomer is unfavourable.

If the stable isomer is invariant for the degenerate dsd's, it will be transformed into itself by these pathways. The present work shows that for such isomers, NMR experiments are in general "dsd compatible". The only exception of this category is the D_{5h} $HMo[P(OCH_3)_3]_4[O_2CCF_3]$, where non-pairwise exchange is preferred in spite of the fact that double degenerate dsd does not lead to isomerization.

It seems interesting to design other dsd invariant substitution patterns in order to confirm these general tendencies.

Acknowledgement

We thank Mr. R. Vandeloise for computer-assisted drawing of the figures.

Appendix: dsd mechanisms of the 4-capped trigonal prism

We use the method described in ref. [8]. Suppression of one or two edges of the 4-capped trigonal prism, #36, leads to polyhedra #38, #40, #42 or #43, #44 respectively [3]. Further edge suppression is meaningless since seven vertex polyhedra have at least eleven edges. It is easy to show that there are no single degenerate dsd of #36. Note that the removal of *one* edge of #36 can lead to a pentagonal face, since #36 has quadrilateral faces. Polyedron #38 has such a pentagonal face. However there is no degenerate 5-pyramidal process [4] for #36.

We could also imagine a process where the removal of an edge is followed by the diagonalisation of one of the faces which were present in the starting polyhedron. We call such a process a dss'd' process, since the square face which is diagona-

lized is different from the square face arising from edge removal. Such a degenerate process exists for #36 (see fig. 17). It is seen on this figure that removal of edge 34 is indeed followed by addition of edge 36 to diagonalize the quadrilateral face 2376 of the original polyhedron. The intermediate polyhedron is # 40.

We now turn our attention to the processes resulting from the removal of two edges. There exist various possibilities arising from the combination of dsd, dss'd' and 5-pyramidal processes. The only sequences resulting in degenerate processes are listed in figs. 18–20.

In fig. 18, a combination of dsd and dss'd' is shown. The quadrilateral face 1374 is the intermediate of the dsd. The dss'd' can be described as the removal of edge 12 in the "diamond" 1523 and addition of edge 46 on the quadrilateral face 4567. Two dss'd' are combined in fig. 19 since the two quadrilateral faces of the starting configuration are diagonalized in the final one, and vice versa. Finally, fig. 20 shows a 5-pyramidal process with 13762 as intermediate pentagonal face combined to a dss'd', where one quadrilateral face of the original configuration is diagonalized in the final one, and vice versa.

It is easy to show that the processes described in fig. 17 to 20 belong to different modes of rearrangements [9–11].

References

[1] E.L. Muetterties and C.M. Wright, Quart. Rev. 21 (1967) 109.
[2] E.L. Muetterties and L.J. Guggenberger, J. Am. Chem. Soc. 96 (1974) 1748.
[3] D. Britton and J.D. Dunitz, Acta Cryst. 29A (1973) 362.
[4] R.B. King, Inorg. Chem. 24 (1985) 1716.
[5] R.B. King, Inorg. Chim. Acta 49 (1981) 237.
[6] W.N. Lipscomb, Science 153 (1966) 373.
[7] D.L. Kepert, *Inorganic Stereochemistry* (Springer, Berlin, 1982).
[8] J. Brocas and M. Bauwin, J. Math. Chem. 6 (1991) 281.
[9] W. Hässelbarth and E. Ruch, Theor. Chim. Acta 29 (1973) 259.
[10] W.G. Klemperer, J. Am. Chem. Soc. 94 (1972) 8360.
[11] J. Brocas, M. Gielen and R. Willem, *The Permutational Approach to Dynamic Stereochemistry* (Mc Graw-Hill, New York, 1983).
[12] R. Davis, M.N.S. Hill, C.E. Holloway, B.F.G. Johnson and K.H. Al-Obaidi, J. Chem. Soc. A (1971) 994.
[13] E.O. Bishop, G. Butler, J. Chatt, J.R. Dilworth, G.J. Leigh, D. Orchard and M.W. Bishop, J. Chem. Soc. Dalton (1978) 1654.
[14] S.L. Hawthorne and R.C. Fay, J. Am. Chem. Soc. 101 (1979) 5268.
[15] M.H. Chisholm, F.A. Cotton and M.W. Extine, Inorg. Chem. 17 (1978) 2000.
[16] P.J. Domaille, B.M. Foxman, T.J. Mc Neese and S.S. Wreford, J. Am. Chem. Soc. 102 (1980) 4114.
[17] B.W. Clare, M.C. Favas, D.L. Kepert and A.S. May, in: *Advances in Dynamic Stereochemistry*, ed. M. Gielen (Freund, Publ., 1985) p. 1.
[18] A.P. Ginsberg and M.E. Tully, J. Am. Chem. Soc. 95 (1973) 4749.
[19] J.O. Albricht, S. Datta, B. Dezube, J.K. Kouba, D.S. Marynick, S.S. Wreford, B.M. Foxman, J. Am. Chem. Soc. 101 (1979) 611.

[20] S.S. Wreford, J.K. Kouba, J.F. Kirner, E.L. Muetterties, I. Tavanaiepour and V.W. Day, J. Am. Chem. Soc. 102 (1980) 1558.
[21] F.A. Van-Catledge, S.D. Ittel, C.A. Tolman and J.P. Jesson, J. Chem. Soc. Chem. Comm. (1980) 254.
[22] F.A. Van-Catledge, S.D. Ittel and J.P. Jesson, Organometallics 4 (1985) 18.
[23] D.J. Klein and A.H. Cowley, J. Am. Chem. Soc. 97 (1975) 1633.
[24] J.G. Nourse, J. Am. Chem. Soc. 102 (1980) 4883.
[25] R.E. Stanton and J.W. McIver, J. Am. Chem. Soc. 97 (1975) 3632.
[26] P. Pechukas, J. Chem. Phys. 64 (1976) 1516.
[27] J. Brocas and R. Willem, J. Am. Chem. Soc. 105 (1983) 2217.
[28] J.T. Hougen, J. Chem. Phys. 37 (1962) 1433.
[29] W.R. Cullen and L.M. Mihichuk, Canad. J. Chem. 54 (1976) 2548.
[30] P. Meakin, L.J. Guggenberger, F.N. Tebbe and J.P. Jesson, Inorg. Chem. 13 (1974) 1025.
[31] S. Datta, B. Dezube, J.K. Kouba and S.S. Wreford, J. Am. Chem. Soc. 100 (1978) 4404.
[32] E.B. Dreyer, C.T. Lam and S.J. Lippard, Inorg. Chem. 18 (1979) 1904.
[33] J.L. Templeton and B.C. Ward, Inorg. Chem. 19 (1980) 1753.
[34] J.L. Templeton and B.C. Ward, J. Am. Chem. Soc. 103 (1981) 3743.
[35] D.F. Lewis and S.J. Lippard, Inorg. Chem. 11 (1972) 621.
[36] C.T. Lam, M. Novotny, D.L. Lewis and S.J. Lippard, Inorg. Chem. 17 (1978) 2127.
[37] S.J. Lippard, Progr. Inorg. Chem. 21 (1978) 91.
[38] J.A. Connor, G.K. McEwen and C.J. Rix, J. Chem. Soc. Dalton Trans. (1974) 589.
[39] L.D. Brown, S. Datta, J.K. Kouba, L.K. Smith and S.S. Wreford, Inorg. Chem. 17 (1978) 729.
[40] K. Henrick and S.B. Wild, J. Chem. Soc. Dalton Trans. (1974) 2500.
[41] R. Hoffmann, B.E. Beier, E.L. Muetterties and A.R. Rossi, Inorg. Chem. 16 (1977) 511.